M. SROKA[1*], A. ZIELIŃSKI[2], T. PUSZCZAŁO[1,3], K. SÓWKA[1,3], B. HADZIMA[4]

STRUCTURE OF 22Cr25NiWCoCu AUSTENITIC STAINLESS STEEL AFTER AGEING

The 22Cr25NiWCoCu austenitic stainless steel was developed by AB Sandvik Material Technology in Sweden. Due to its high creep strength and good corrosion resistance, this material is well suited for use in superheaters in advanced coal-fired power boilers as well as in other types of steam boilers using various types of fuel. The examined material was subject to long-term ageing for the time of annealing up to 20 000 h at 700 and 750°C. Precipitation processes and microstructure stability as-received and after ageing were investigated. Examination of the microstructure was conducted using scanning electron microscopy. The identification of secondary phases was carried out by X-ray phase composition.

Using the results of the investigations of precipitation processes in the microstructure, both within the grains and at the grain boundaries, their statistical analysis was carried out. To illustrate this impact, the following parameters were used: surface area and equivalent diameter of precipitates. Based on the surface area measurements, the percentage of the phase in the reviewed photo's total area was calculated.

Keywords: 22Cr25NiWCoCu steel; microstructure; precipitates; ageing

1. Introduction

The development of power engineering in Poland may be continued based on the national hard and brown coal resources or more or less support from nuclear power engineering and renewable energy engineering. The amendments to the energy legislation confirm the concerns of entrepreneurs from the renewable energy sector and environmental organisations that the development of traditional energy, including gas power stations, is still promoted for various economic and social reasons. This may cause Poland to fail to meet the international and EU environmental and climate protection commitments and may also result in problems of preserving the country's energy security [1-9].

Technologies that generate energy in a stable and predictable way, which exclude wind power plants, will be promoted to a greater extent. It may turn out that renewable energy will be produced in a significant part of coal-fired power plants by the so-called co-firing of wood. In addition to co-firing, we can also count on energy production from biogas and photovoltaic farms. In addition, the construction of a Polish offshore wind farm is planned [10-17].

At present, the power grid in Poland is old and generally degraded. Therefore heavy investments in energy engineering are required with regard to the modernisation of power units and transmission lines, which also operate at the verge of capacity. This makes it necessary to launch large-scale research into materials intended for elevated and high-temperature applications [18-23]. Materials used for equipment in the power industry should have good properties under prolonged exposure to heat, stress and corrosive environments. The 22Cr25NiWCoCu steel is now one of the best materials that can be used in components of supercritical boilers operating under the toughest temperature and stress conditions. Due to its high creep strength and good corrosion resistance, this material is well suited for superheaters in advanced coal-fired power boilers. The subject of the investigations in this paper was the statistical analysis of precipitation processes in the test steel microstructure during long-term ageing.

1   SILESIAN UNIVERSITY OF TECHNOLOGY, DEPARTMENT OF ENGINEERING MATERIALS AND BIOMATERIALS, S. KONARSKIEGO 18A, 44-100 GLIWICE, POLAND
2   ŁUKASIEWICZ RESEARCH NETWORK – INSTITUTE FOR FERROUS METALLURGY, K. MIARKI 12-14, 44-100 GLIWICE, POLAND
3   ZRE, UL. GEN. JANKEGO 13, 40-615 KATOWICE, POLAND
4   UNIVERSITY OF ŽILINA, UNIVERZITNÁ 8215/1, 010 26 ŽILINA, SLOVAKIA

*   Corresponding author: marek.sroka@polsl.pl

TABLE 1

Chemical composition of the 2Cr25NiWCoCu steel, wt %

Chemical composition [wt %]											
C	Si	Mn	P	S	Cu	Cr	Ni	W	Co	Nb	B
0.06	0.25	0.50	0.01	<0.01	2.9	23.0	24.1	3.2	1.4	0.4	0.005

2. Material for research

The research subjects were sections of superheater coils with dimensions of ø 38 × 8.8 mm made of heat-resistant austenitic 2Cr25NiWCoCu steel. The chemical composition of the test steel is presented in Table 1.

22Cr25NiWCoCu steel with approx. 22% chromium, 24% nickel, 3% tungsten with the addition of copper and cobalt capable of operating within ultra-supercritical steam parameters (up to 700°C). The examined material was subject to long-term ageing for the time of annealing up to 20 000 h at 700 and 750°C.

3. Test results

In the as-received condition, the microstructure of the test steel only showed the primary precipitates which were observed within the grains (Fig. 1), but no precipitates were observed at the grain boundaries. The ageing process of a solution-heat treated steel results in the precipitation of secondary phases. The secondary phase precipitates at the grain boundaries and precipitates within the grains are present in the microstructure of the 22Cr25NiWCoCu steel after ageing. During the initial ageing period, there is a visible precipitation process in the test steel, which intensifies with an increase in the ageing time. In the test steel after 1000 h ageing at 700 and 750°C, the $M_{23}C_6$ carbides
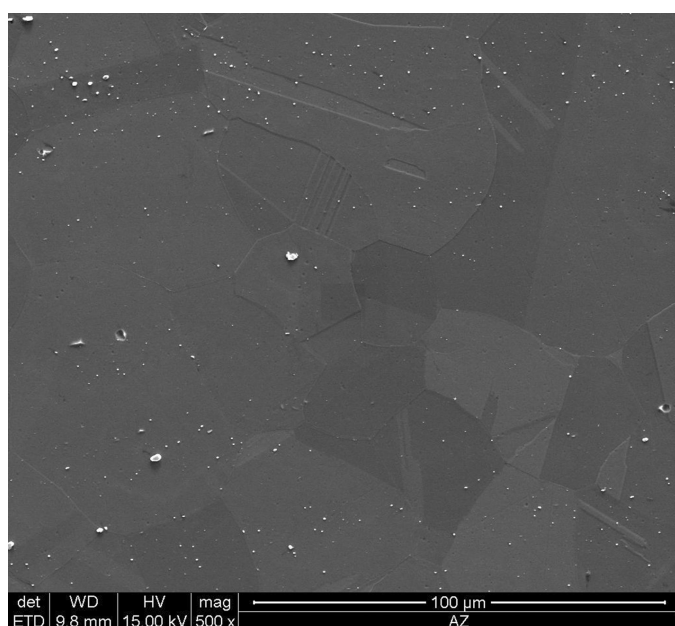

Fig. 1. Microstructure of 22Cr25NiWCoCu steel in as-received condition, SEM

and fine Laves phase precipitates (Fe_2W) were identified at the grain boundaries. Longer ageing times result in the occurrence of particles of the σ phase at the grain boundary (Fig. 2). The amount and size of precipitates of this phase increase with the extension of ageing time, which results from the high coagulability of the σ phase.

Using the results of the investigations of precipitation processes in the microstructure of the 22Cr25NiWCoCu steel, both within the grains and at the grain boundaries, their statistical analysis was carried out. The results of mechanical tests [24-26] indicate that these precipitates significantly impact the properties of the test material. To illustrate this impact, the following parameters were used: surface area and equivalent diameter of precipitates.

The quantitative analysis of precipitates was performed using a computer-based image analysis system, based on the microstructure images acquired with a scanning electron microscope at 2000× magnification. The image analysis system was calibrated to the scale marker on the microstructure images. A fixed measurement frame of 1020 × 940 pixels was used. An example workflow used during the image analysis to extract the analysed phase precipitates is shown in Fig. 3. Based on the surface area measurements, the percentage of the phase in the reviewed photo's total area was calculated. In order to clearly define the average size of a particle from a set of particles, the average diameter equivalent to the area of particles in the that set was determined.

When calculating the surface area and equivalent diameter, the focus was placed on the $M_{23}C_6$, Laves phase and σ phase precipitates, the calculation of which was possible using the images of microstructure obtained from the scanning electron microscope. The calculated statistical measures describing the empirical distributions of the equivalent diameter of the precipitates.

The $M_{23}C_6$ carbides have relatively low thermal stability, which results in an increase in the size of these precipitates with the extension of ageing time (Fig. 4), whereas the percentage of $M_{23}C_6$ carbides decreases with the passage of ageing time (Fig. 5), which is caused by their absorption due to growth of the σ phase.

With elapse of the time of ageing at both 700 and 750°C, the percentage and average diameter of the Laves phase precipitates increases (Figs. 6, 7). The Laves phase is a more efficient and stable precipitate than $M_{23}C_6$ carbide. The Laves phase effect precipitated within the grains on the steel properties depends on its size and volume fraction.

The precipitation of σ phase in austenitic steels is much slower than that of $M_{23}C_6$ carbides because the preferred pre-
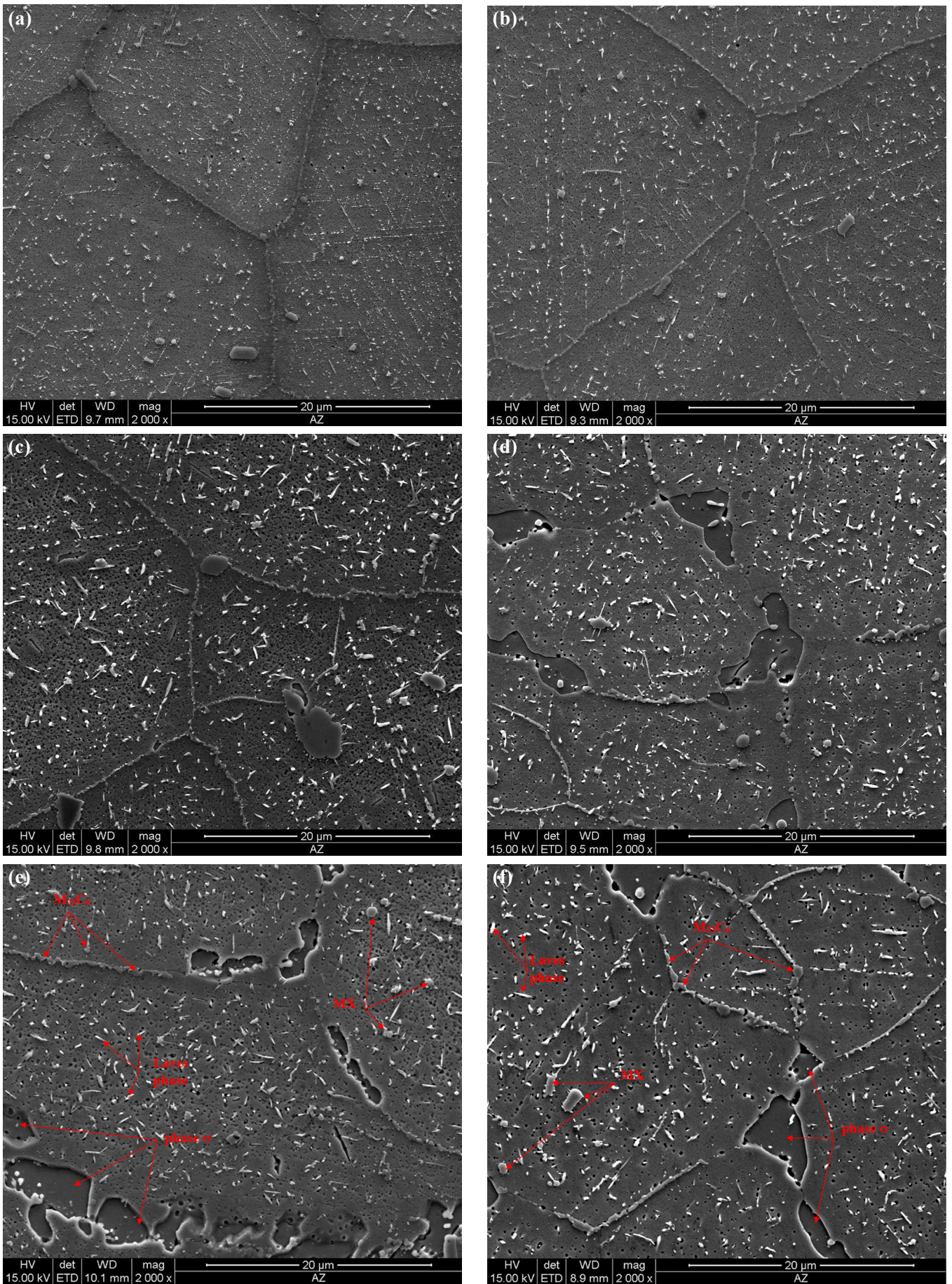
Fig. 2. Microstructure of 22Cr25NiWCoCu steel after ageing at (a) 700°C/1000 h, (b) 750°C/1000 h, (c) 700°C/10 000 h, (d) 750°C/10 000 h, (e) 700°C/20 000 h, (f) 750°C/20 000 h, SEM
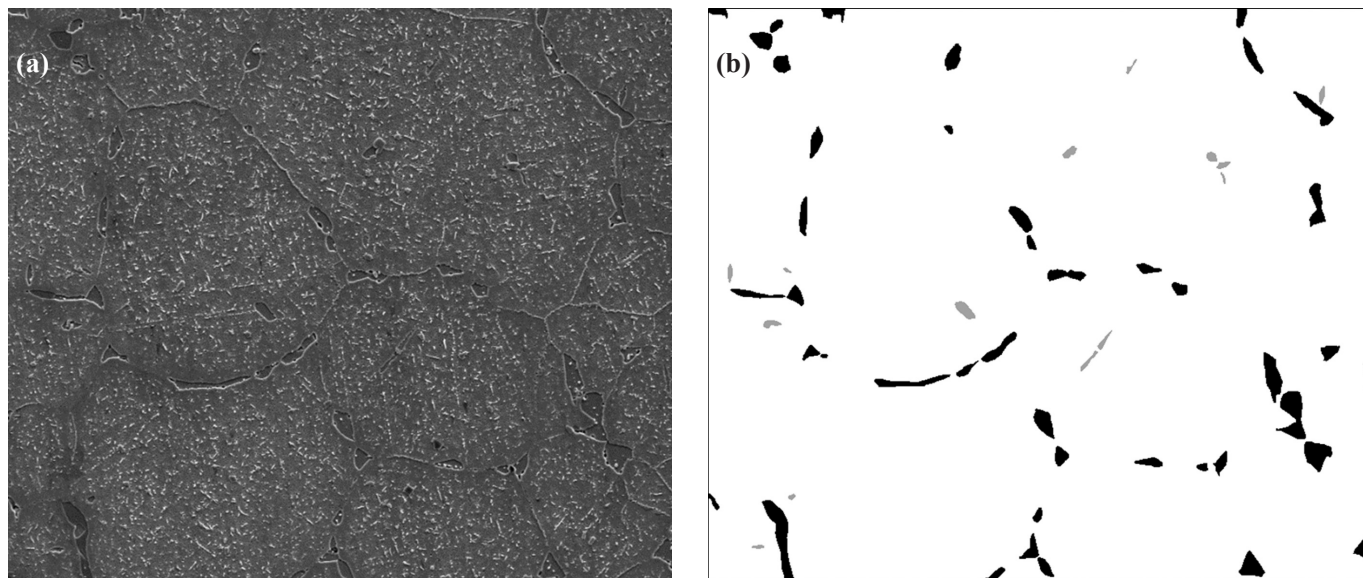
Fig. 3. Image analysis of σ phase precipitates of the 22Cr25NiWCoCu steel after 20 000 h of ageing at 750°C; a) original image, b) binary image
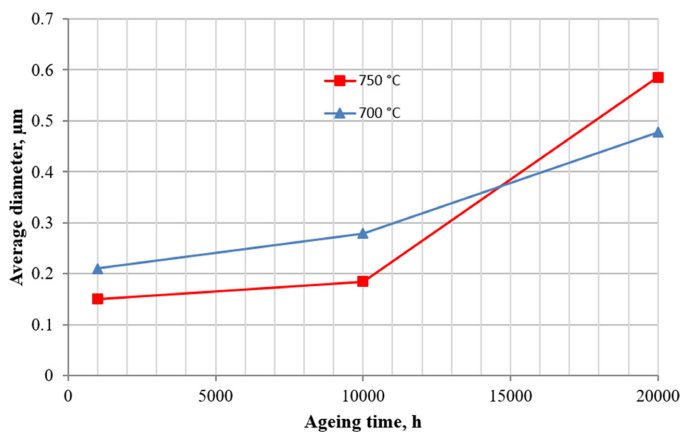

Fig. 4. Results of the quantitative analysis of the equivalent diameter of $M_{23}C_6$ precipitates after 20 000 h of ageing
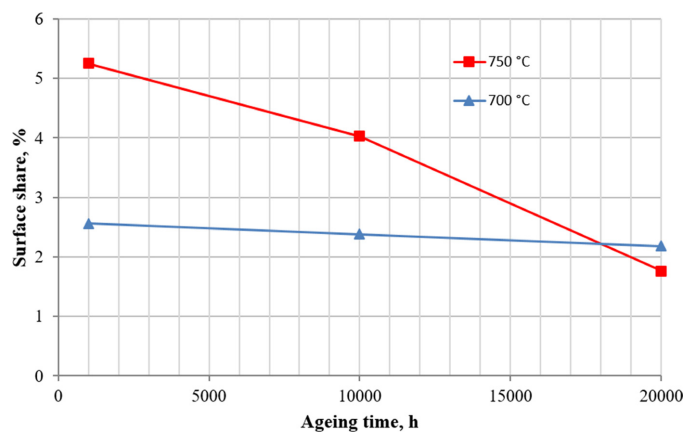

Fig. 5. Results of the quantitative analysis of the surface area of $M_{23}C_6$ precipitates after 20 000 h of ageing
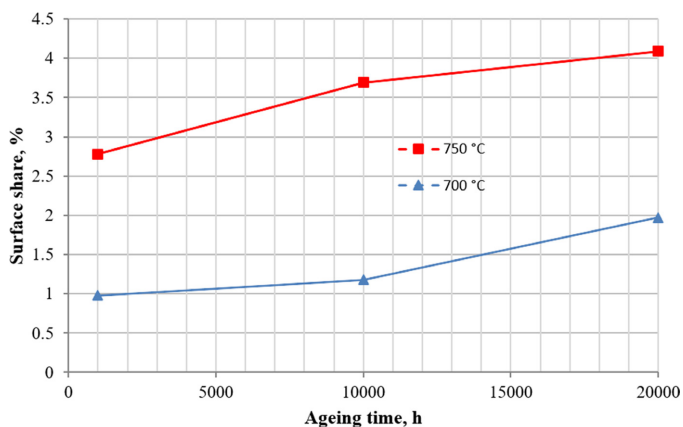

Fig. 6. Results of the quantitative analysis of the equivalent diameter of Laves phase after 20 000 h of ageing
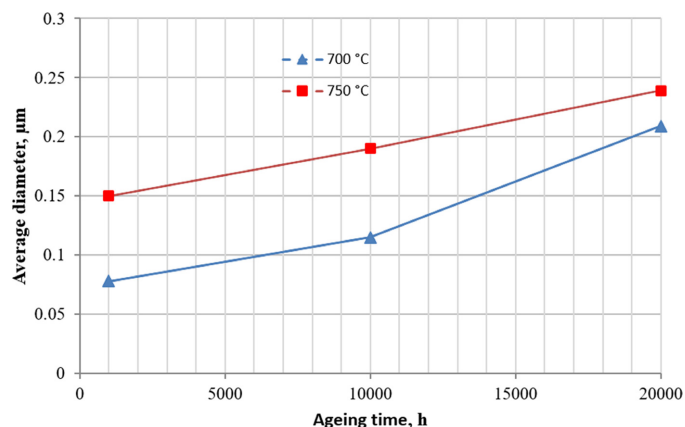

Fig. 7. Results of the quantitative analysis of the surface area of Laves phase after 20 000 h of ageing

cipitation processes are the formation of carbides and/or nitrides. It is mainly due to the fact that the diffusion of chromium in austenite takes place very slowly, the σ phase precipitates in austenite are non-coherent precipitates with matrix and, in addition, the solubility of carbon and nitrogen in austenite is low [27]. With elapse of the time of ageing at both 700 and 750°C,
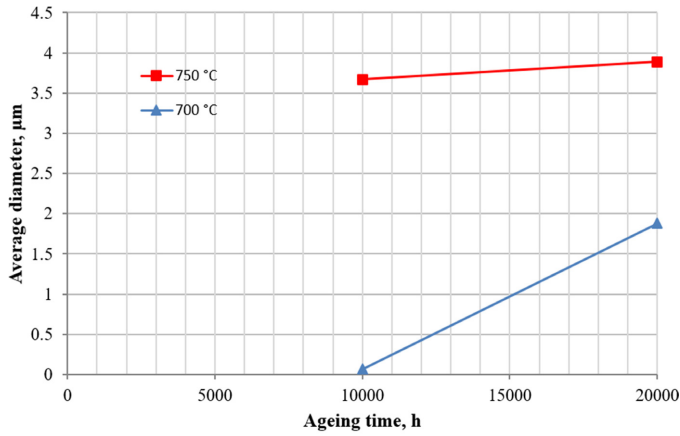
Fig. 8. Results of the quantitative analysis of the equivalent diameter of σ phase after 20 000 h of ageing
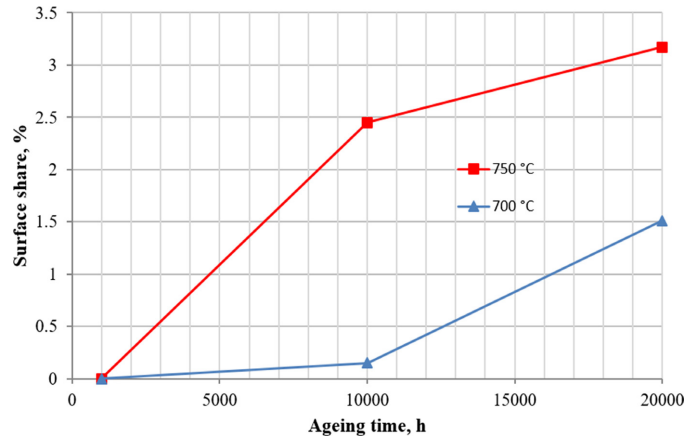

Fig. 9. Results of the quantitative analysis of the surface area of σ phase after 20 000 h of ageing

the percentage and average diameter of the σ phase precipitates increases (Figs. 8, 9).

The histograms of the distribution of the average diameter equivalent to the size of precipitates of the analysed phases and the selected histograms describing the distribution of the surface area of the analysed phases for the most characteristic states of the material are shown in Fig. 10 for $M_{23}C_6$ precipitates, Fig. 11 for Laves phase precipitates and Fig. 12 for σ phase precipitates, respectively, in the test steel after 20 000 h ageing at 700°C.

4. Summary

The obtained results confirm the observations of the microstructure that show a higher share of the σ phase in the materials aged at 750°C than in those aged at 700°C and a higher level of the σ phase precipitates at 750°C.

Compared to the currently commercially available austenitic heat resistant steels that can be used at up to 650°C and the nickel alloys that can be used above this temperature, which
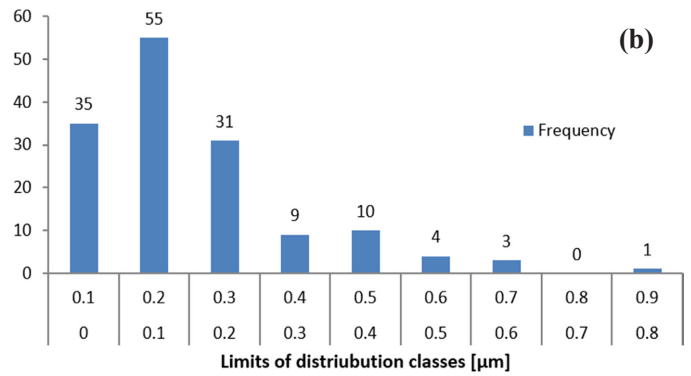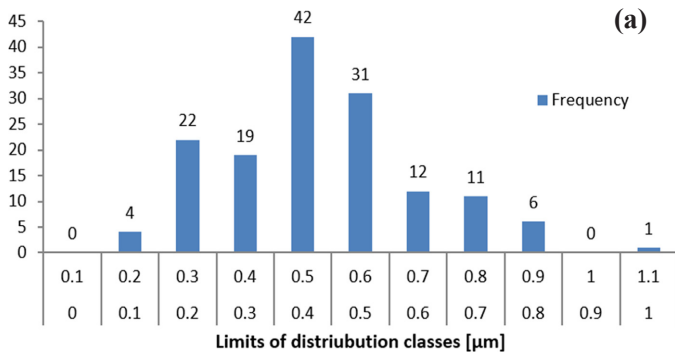

Fig. 10. Histograms of the distribution of the average diameter (a) and surface area (b) of $M_{23}C_6$ precipitates after 20 000 h of ageing
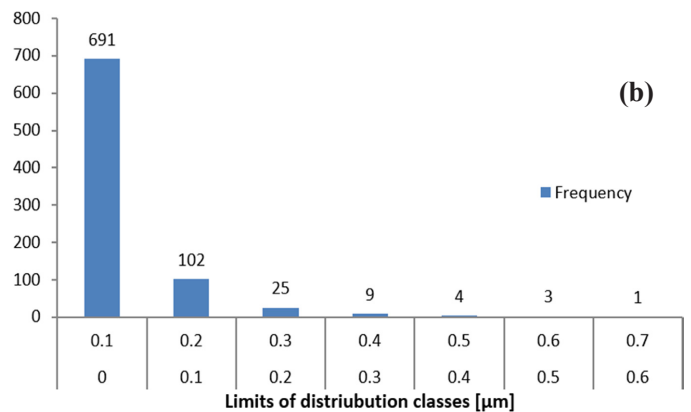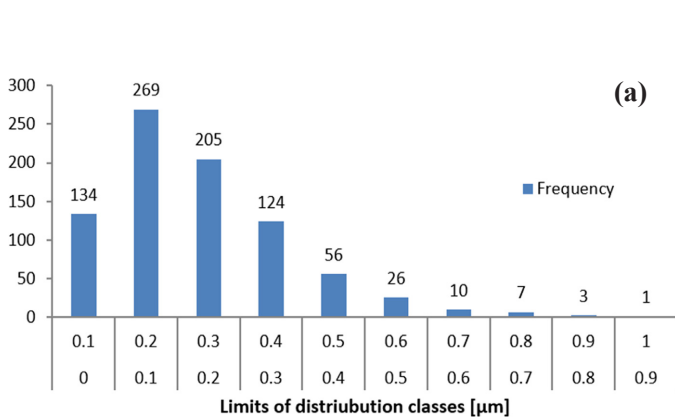

Fig. 11. Histograms of the distribution of the average diameter (a) and surface area (b) of Laves phase after 20 000 h of ageing
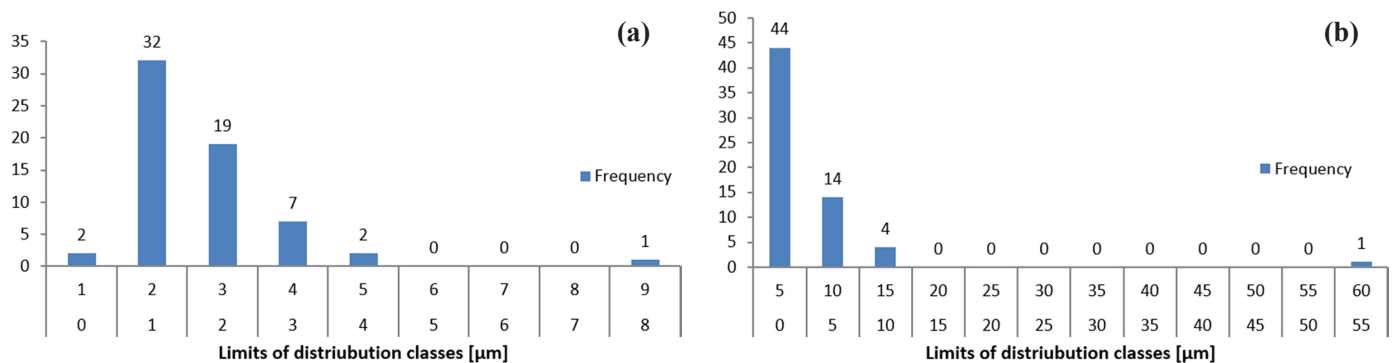
Fig. 12. Histograms of the distribution of the average diameter (a) and surface area (b) of σ phase after 20 000 h of ageing

are however significantly more expensive, the test steel is an alternative the application of which may reduce the investment cost of the whole boiler.

The results of the described investigations are not only of practical significance. Still, they can also be used in the diagnostic activities for the assessment of the critical components of the pressure part of power boilers working above the limit temperature, which is particularly valuable from the application point of view in estimating the time of safe service of the test materials. This is also of great importance with a view to the introduction of the test steel into the Polish power industry and may provide a knowledge base for the development of degradation processes of the test steels' microstructure and properties in forecasting their service life.

REFERENCES

[1] L. Sozańska-Jędrasik, J. Mazurkiewicz, K. Matus, W. Borek, Materials **13**, 739 (2020).

[2] A. Zieliński, M. Sroka, T. Dudziak, Materials **11**, 2130 (2018).

[3] P. Barnard, Austenitic steel grades for boilers in ultra-supercritical power plants, in: A. Di Gianfrancesco (Eds.), Materials for ultra-supercritical and advanced ultra-supercritical power plants, Woodhead Publishing (2017).

[4] M. Kremzer, M. Dziekońska, M. Sroka, B. Tomiczek, Arch. Metall. Mater. **61** (3), 1255-1260 (2016).

[5] M. Król, T. Tański, W. Sitek, Thermal analysis and microstructural characterization of Mg-Al-Zn system alloys, in: E. Oanta, R. Comaneci, C. Carausu, M. Placzek, V. Cohal, P. Topala, D. Nedelcu (Eds.), Modern technologies in industrial engineering, Institute of Physics Publishing (2015).

[6] L.W. Żukowska, A. Śliwa, J. Mikuła, M. Bonek, W. Kwaśny, M. Sroka, D. Pakuła, Arch. Metall. Mater. **61** (1), 149-152 (2016).

[7] M. Sroka, M. Nabiałek, M. Szota, A. Zieliński, Rev. Chim-Bucharest. **4**, 737-741 (2017).

[8] S. Zhang, Z. Jiang, Mater. Charact. **137**, 244-255 (2018).

[9] X.Y. San, B. Zhang, Corros. Sci. **130**, 1609-1616 (2017).

[10] M. Król, J. Therm. Anal. Calorim. **133** (1), 237246 (2018).

[11] M. Sroka, A. Zieliński, J. Mikuła, Arch. Metall. Mater. **61** (3), 969-974 (2016).

[12] L.A. Dobrzański, W. Borek, J. Mazurkiewicz, Arch. Metall. Mater. **61** (2), 725-730 (2016).

[13] J. Horvath, J. Janovec, M. Junek, Sol. St. Phen. **258**, 639-642 (2017).

[14] J.W. Bai, P.P. Liu, Y.M. Zhu, X.M. Li, C.Y. Chi, H.Y. Yu, X.S. Xie, Q. Zhan, Mat. Sci. Eng. A-Struct. **584**, 57-62 (2013).

[15] W. Borek, T. Tański, Z. Jonsta, P. Jonsta, L. Cizek, in Proc. METAL 2015: 24th International Conference on Metallurgy and Materials, (2015).

[16] A. Zieliński, M. Miczka, M. Sroka, Mater. Sci. Tech-Lond. **32** (18), 1899-1910 (2016).

[17] A.F. Padilha, P.R. Rios, ISIJ Intern. **42** (4), 325-327 (2002).

[18] T. Tokairin, K.V. Dahl, H.K. Danielsen, F.B. Grumsen, T. Sato, J. Hald, Mat. Sci. Eng. A-Struct. **565**, 285-291 (2013).

[19] Q. Zhou, R. Wang, Z. Zheng, Y. Gao, Appl. Surf. Sci. **462**, 804-814 (2018).

[20] L. Sozańska-Jędrasik, J. Mazurkiewicz, W. Borek, K. Matus, Arch. Metall. Mater. **63** (1), 265-276 (2018).

[21] G. Golański, A. Zieliński, A. Zielińska-Lipiec, Materialwiss. Werkst. **46** (3), 248-25 (2015).

[22] L.A. Dobrzański, M. Kremzer, K. Gołombek, Mater. Sci. Forum **591-593**, 188-192 (2008).

[23] P. Snopiński, T. Tański, M. Sroka, M. Kremzer, Metalurgija **56** (3-4), 329-332 (2017).

[24] A. Zieliński, G. Golański, M. Sroka, Mat. Sci. Eng. A-Struct. **796**, 139944 (2020).

[25] R.L. Plaut, C. Herrera, D.M. Escriba, P.R. Rios, A.F. Padilha, Mater. Res. **10** (4), 453-460 (2007).

[26] M. Sroka, A. Zieliński, G. Golański, T. Puszczało, J. Zacłona, Acta Phys. Pol. A **138** (2), 232-235 (2020).

[27] G. Golański, Żarowytrzymałe stale austenityczne, Wydawnictwo Wydziału Inżynierii Produkcji i Technologii Materiałów, Politechniki Częstochowskiej (2017).